Influence of Al^{3+} substitution on impedance spectroscopy studies of $Ni_{0.27}Cu_{0.10}Zn_{0.63}Al_xFe_{2-x}O_4$

M. Belal Hossen[1*], A.K.M. Akther Hossain[2]

[1]*Department of Physics, Chittagong University of Engineering and Technology, Chittagong, Bangladesh*
[2]*Department of Physics, Bangladesh University of Engineering and Technology, Dhaka, Bangladesh*

*Corresponding author. Tel: (+88) 0193665367; E-mail: belalcuet@gmail.com

ABSTRACT

The influence of Al^{3+} substitution on the microstructure and impedance spectroscopy of $Ni_{0.27}Cu_{0.10}Zn_{0.63}Al_xFe_{2-x}O_4$ has been studied by scanning electron microscopy and impedance analyzer where the formation of the material in the spinel crystal structure was initially confirmed by X-ray structural analysis with room temperature data. The surface morphology indicates well defined grains separated by grain boundaries and with Al substitution average grain size decrease from 17 µm to 12 µm and zinc losses as well. The complex-plane impedance spectra indicate that the material can be represented by two semicircular arcs (its tendency) which corresponds to the bulk and the grain boundary resistance at high and low frequencies respectively. With Al substitution both grain and grain boundary resistance increases from 7.48 kΩ to 15.62 kΩ and 92.34 kΩ to 192.46 k respectively. Electric modulus spectra reflect the contributions from grain and grain boundary effects: the large resolved semicircle arc caused by the grain effect and the small poorly resolved semicircle arc was attributed to the grain boundary. Copyright © 2015 VBRI Press.

Keywords: Surface morphology; impedance spectroscopy; enhanced grain and grain boundary resistance; resolve relaxation.

Introduction

Soft ferrites with spinel structure are magnetic materials with a general formula $Me'Fe_{2-\partial}Me''_{\partial}O_4$, in which Me' represents a divalent cation ($Me' = Ni^{2+}$, Cu^{2+}, Zn^{2+}, Cd^{2+}, Mn^{2+}), or a combination of cations with an average valency of two, and Me'' a trivalent cation ($Me'' = In^{3+}$, Al^{3+}, Cr^{3+}, Y^{3+}, La^{3+}, Sm^{3+}), or a combination of cations with an average valency of three. The composition parameter (∂) can range between zero and two, but it is obvious that if ∂ is close to two, these oxides cannot be considered anymore as ferrites [1]. These cations are distributed at the tetrahedral (A) and octahedral (B) available sites in AB_2O_4 spinel lattice. The magnetic and electric properties of a spinel ferrite are sensitive to the types of cations and their distribution amongst the two interstitial sites of spinel lattice [2]. Apart from the magnetic properties, studies of electric and dielectric behavior are equally important from both fundamental and applied point of view. Polycrystalline ferrites are very good dielectric materials and have many technological applications ranging from microwave to radio frequencies. The high permeability and low electrical conductivity in such materials are very useful for inductor, transformer cores, switch mode power supplies, rotary transformers, noise filters, and multilayer ferrite chip components [3, 4]. The variation of conductivity greatly

influences the dielectric and magnetic behavior of ferrites and is mostly dependent on the composition, preparation method and sintering condition [5, 6]. It has been reported earlier that ferrites sintered in air are highly characterized by conducting grains separated by poorly conducting grain boundaries [7].

Complex impedance spectroscopy (CIS) is a useful, well-designed and nondestructive method [8] to study the microstructural and electrical properties of polycrystalline oxides. This can correlate the structural and electrical characteristics of polycrystalline oxides in a wide range of frequencies and temperatures. CIS also describes the electrical processes occurring in a system by applying an ac signal as input perturbation, which helps to separate the contribution of electroactive regions (such as grain boundary and grain effects). The output response, when plotted in a complex plane plot, appears in the form of succession of semicircles representing electrical phenomena due to the bulk material, grain boundary effect and interfacial polarization [9]. Several researchers [9-12] have synthesized various ceramics and studies the structure-microstructure related impedance properties. For Zn substituted $Ni_{0.7-x}Zn_xCu_{0.3}Fe_2O_4$ ferrites, it is observed that the electrical properties such as dielectric constant and loss tangent both show a normal behavior with respect to frequency. The dielectric and ac conductivity parameters

show their maximum value for 10% Zn-doping composition [**13**]. Due to combined effect of electrical and magnetic properties of ferrites, they are good candidate as multiferroic materials. Recently, Kumar et al. have reported that ferrites also behave like multiferroics [**14**]. Hashim *et al.* [**15**] have successfully synthesized single phase $Ni_{0.7}Zn_{0.3}Al_xFe_{2-x}O_4$ ($0.0 \leq x \leq 0.5$) nanoparticles using chemical route. The complex impedance measurements show two semicircles for all the samples, which shows that the resistive and the capacitive properties of the samples are associated with the grain and grain boundaries. Also the dielectric loss of Al^{3+} substituted NiCuZn was found to decrease with Al^{3+} ion content [**16**].

However, reports have been found in the literature on electric modulus (dielectric feature) and impedance spectroscopy of Al substituted mixed NiCuZn ferrites is scarce. This material has extensively been studied due to its high resistivity. So the analysis in order to know the source of resistance, contribution of resistances from grains and grain boundaries, to resolves the relaxation contributions and conduction phenomenon in them is more intriguing. With these motivations we aimed at understanding the electrical properties of Al substituted $Ni_{0.27}Cu_{0.10}Zn_{0.63}Al_xFe_{2-x}O_4$. As per the best of our knowledge, researchers had tried to investigate, analyze, and understand the anomalous properties (i.e. structural, electrical, dielectric etc.) of ferrites using different experimental technique but an adequate analysis of impedance spectroscopy and electric modulus of Al substituted ferrites is still lacking and offers further investigations.

Experimental

Material Synthesis

$Ni_{0.27}Cu_{0.10}Zn_{0.63}Al_xFe_{2-x}O_4$ ($0 \leq x \leq 0.12$ with step of 0.04) bulk samples were prepared using high temperature sintering environment where as the initial powders were synthesized by auto combustion method. High purity 'AR' grade raw materials of ($Ni(NO_3)_2.6H_2O$, $Cu(NO_3)_2.3H_2O$, $Zn(NO_3)_2.6H_2O$, $Fe(NO_3)_3.9H_2O$ and $Al(NO_3)_3.9H_2O$) were mixed together according to their required stoichiometry. These ingredients were first mixed using minimum amount of ethanol thoroughly using a magnetic stirrer at 70°C. The mixed solution was then evaporated on a constant temperature water bath. After boiling and ignition of the mixture, a spinel residue is obtained in a few minutes. These powders are crushed and grounded thoroughly. The mixture of the composition was ground to a very fine powder, and calcined at 700°C for 5h. Following the addition of polyvinyl alcohol (PVA), the milled powders were granulated and pressed into pellets shaped which were finally sintered at 1300°C for 5h in air. The temperature ramp for calcinations and sintering was 10°C/min for heating, and 5°C/min for cooling.

Characterizations

After sintering microstructure and surface morphology of the samples have examined by scanning electron microscope (SEM). The X-ray density as calculated using the relation, $\rho_X = (8M_A)/(N_Aa^3)$; where N_A is Avogadro's number and M_A is the molecular weight of the composition

and ρ_B (mass/volume) is the bulk density. The structural characterization was performed by X-ray diffraction (XRD) studies using a RIGAKU smart-lab diffractometer with Cu-Kα radiation. Frequency dependent dielectric measurements of the present samples were measured by the Waynekerr impedance analyzer (model no. 6500B) works over the wide range of frequency (20 Hz – 120 MHz). For dielectric measurements sintered pellets were polished with fine grained sand paper and coated with high purity silver paste on adjacent faces as electrodes and then dried for 2 h at 150°C to make the parallel plate capacitor geometry.

The real (Z') and imaginary (Z'') parts of impedance were calculated using the relation:

$$Z'' = Z \cos\theta \text{ and } Z'' = Z \sin\theta$$

The real (M') and imaginary (M'') parts of complex electric modulus in terms of real (ε') and imaginary (ε'') parts of dielectric constant were calculated using the relation:

$$M' = \varepsilon'/(\varepsilon'^2 + \varepsilon''^2) \text{ and } M'' = \varepsilon''/(\varepsilon'^2 + \varepsilon''^2)$$

The drive voltage of the Impedance Analyzer used in the present work is 0.5 V.

Results and discussion

The XRD patterns for the samples $Ni_{0.27}Cu_{0.10}Zn_{0.63}Al_xFe_{2-x}O_4$; with x = 0.00, 0.04, 0.08 and 0.12 are shown in **Fig. 1**. Analyzing the XRD patterns, it was observed that the positions of the peaks comply with the reported values [**17**] and with no extra lines, indicating thereby that the samples have a single phase cubic spinel structure.

The lattice constant calculated using Nelson-Riley extrapolation technique was found to decrease from 8.409 Å to 8.390 Å (**Table 1**) with increase in Al^{3+} content. The decrease in lattice constant with increase in Al^{3+} content can be explained on the basis of difference in the ionic radii of Fe and Al ions, since, the ionic radius of Al^{3+} (0.575 Å) is smaller than that of Fe^{3+} (0.635 Å). The variation in the ρ_X and ρ_B with Al^{3+} ion content is shown in **Table 1**. It is clear from the table that the ρ_X and ρ_B decrease with the increase of Al^{3+} content.
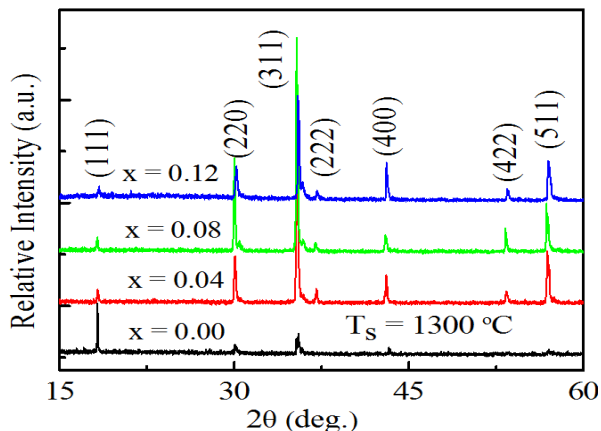
Fig. 1. XRD patterns of $Ni_{0.27}Cu_{0.10}Zn_{0.63}Al_xFe_{2-x}O_4$ with x = 0.00, 0.04, 0.08 and 0.12.

With the intention of understand the surface morphology, grain shape and grain size of as sintered samples (without polishing and etching), SEM study was carried out. **Fig. 2** represents the SEM images of pure and Al substituted ferrite samples sintered at $1300°C$ for 5 h. From the micrograph it is clear that sintered samples results in greater densification with less porosity except for pure NiCuZn ferrite. The grain size in exposed surface for x = 0.00 is disappeared. This may be zinc loss due to volatilization at higher sintering temperatures [18]. The average grain size, D_m was gradually decreases with the increasing Al content listed in **Table 1**. The change in grain size as well as grain boundary significantly influence to the impedance and electric modulus spectroscopy.
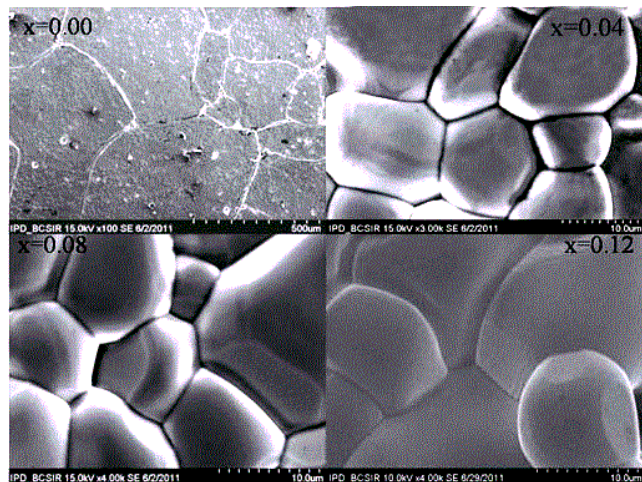
Fig. 2. SEM micrographs for various $Ni_{0.27}Cu_{0.10}Zn_{0.63}Al_xFe_{2-x}O_4$; for (a) x = 0.00, (b) x= 0.04, (c) x = 0.08 and (d) x = 0.12 sintered at $1300°C$.

Table 1. The lattice constant (a_0), density (X-ray, α_X and bulk, α_B), average grain size (D_m) of the various $Ni_{0.27}Cu_{0.10}Zn_{0.63}Al_xFe_{2-x}O_4$ sintered at various temperatures with fixed dwell time 5h.

Content, x	a_0 (Å)	$\rho_X \times 10^3$ (kg/m^3)	$\rho_B \times 10^3$ (kg/m^3)	D_m (μm)
0.00	8.409	5.34	4.51	17
0.04	8.402	5.33	4.32	14
0.08	8.396	5.32	4.27	12
0.12	8.390	5.30	4.19	12

Frequency dependence of the M' of Al substituted $Ni_{0.27}Cu_{0.10}Zn_{0.63}Al_xFe_{2-x}O_4$ are shown in **Fig. 3**. The value of M' is found to be very low at low frequencies and it increases with the increase in frequency. This continuous dispersion on increasing frequency may be contributed to the conduction phenomena due to short range mobility of charge carriers where M' become independent of frequency. It is also found that the dispersion region shifts towards higher frequency side which suggests the long-range mobility of charge carriers [19]. The plateau region observed at higher frequencies suggests about the frequency invariant electrical properties of the materials. The value of M' is found to be dependent on the Al content. The variation of M'' as a function of frequency at various Al content is shown inset of **Fig. 3**. M'' possessed a low value at low frequencies (<10 kHz) for all

compositions. This is probably due to the large value of capacitance at low frequencies. On the other hand, at higher frequencies, well-defined relaxation peaks were clearly observed. The position of the relaxation peak separates the long range hopping region (below the peak frequency) to the short range hopping (above the peak frequency) which varies with Al content. The high frequency side of the peak suggests the confinement of ions in their potential well. The observed asymmetry in peak broadening indicates the spread of relaxation time with different time constant which supports the non-Debye type of relaxation in the materials. With the increase in Al content the peaks are shifting towards higher frequency side indicates that Al substituting activated behavior of relaxation time. The low value of M'' observed at lower frequencies may occur due to the absence of electrode polarization phenomena.
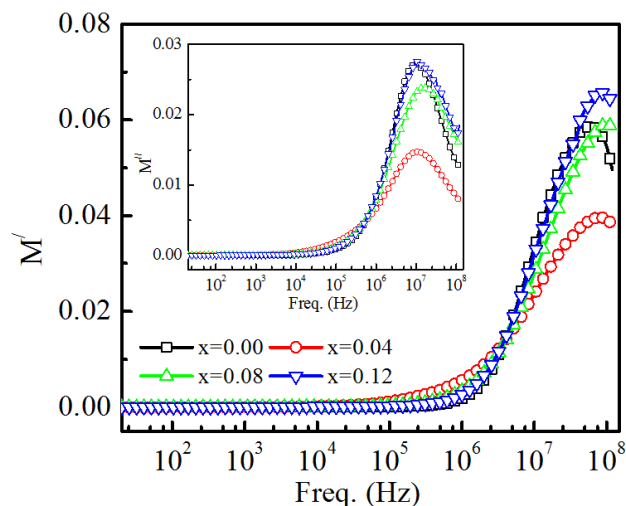
Fig. 3. Frequency dependence of M' and M'' (inset) of $Ni_{0.27}Cu_{0.10}Zn_{0.63}Al_xFe_{2-x}O_4$ with x = 0.00, 0.04, 0.08 and 0.12.
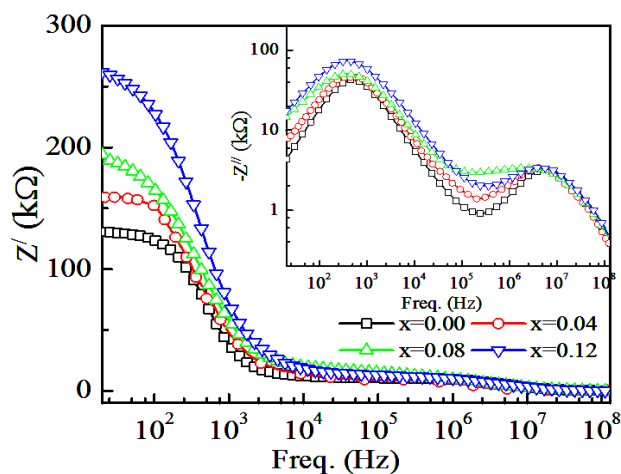
The modulus plots of M'' versus M' for various composition shown in **Fig. 4**. Inset of **Fig. 4** shows low frequency region modulus plot due to the grain boundary contribution.
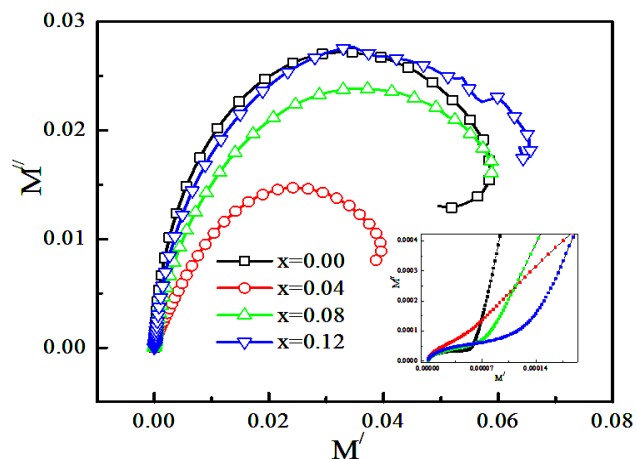
Fig. 4. Frequency dependence M''-M' of $Ni_{0.27}Cu_{0.10}Zn_{0.63}Al_xFe_{2-x}O_4$ with x = 0.00, 0.04, 0.08 and 0.12.

The large semicircle was believed to be induced by the grain effect, due to the smaller capacitance value dominated in the electric modulus spectra, while the small semicircle might be attributed to the grain boundary effect. The form of two deformed semi-circles (or their tendency) with their centers lying below the real axis. This indicates spread of relaxation with different (mean) time constant and hence again supports the non-Debye type of relaxation in the materials. The two semicircular arcs or their tendency in the complex modulus plots suggest the presence of both the grain and grain boundary contributions in these ferrites. It is based on the fact that the impedance plot highlights the phenomenon with the largest resistance whereas modulus plot picks out those of the smallest capacitance. With the huge difference (orders of magnitude) between the resistive values of grains and grain boundaries, it is difficult to obtain two full semicircles for grains and grain boundary on the same scale in the impedance plot. Complex modulus analysis is suitable when materials have nearly similar resistance but different capacitance [20].

Fig. 5 shows the variation of Z' with frequency for $Ni_{0.27}Cu_{0.10}Zn_{0.63}Al_xFe_{2-x}O_4$ at room temperature. On increasing frequency the value of Z' shows steps like decrement which indicates the increase in ac conductivity. At higher frequency, the Z' value merge for all the compositions, which clearly indicate the absence of space charge polarization [21]. The higher impedance value at lower frequency is also an indication of the space charge polarization of the materials. It is observed that Z' increases as the Al content increases in the samples. The behavior can be explained on the basis that with the Al substitution the grain size decreases. This is due to the form of Al_2O_3 layer at the grain boundary which inhibits the grain growth mechanism. The formation of Al_2O_3 at the grain boundary increases resistance significantly in the low frequency region.

increasing Al content, which indicates the presence of composition dependent electrical relaxation phenomenon in the system. The asymmetric broadening of the peaks suggested the presence of electrical processes in the material with a spread of relaxation time [22]. The relaxation phenomenon in the material may be due to the presence of immobile species/electron at low frequencies and in the intermediate frequency range relaxation phenomenon is due to the grain contribution. There was a clear dispersion of the resultant curves in the low and intermediate frequency region at various Al content and appears to be merging at higher frequency irrespective of composition. This behavior may be because of the presence of the space charge polarization effect at lower frequencies, which is eliminated at higher frequencies [23].

The occurrence of relaxation peaks in the Z'' of the complex impedance at low frequency range might be due to the existence of the space–charge layer in the sample composition. Space–charge polarization mechanism is known to predominate in heterogeneous structures, where a material is assumed to be composed of different regions (grain and grain boundaries). The two phases have different electrical conductivity and thus accumulation of charges will be occurred at the grain boundary. These point charges result in an additional space charge polarization i.e. Maxwell–Wagner relaxation in the frequency range (10 Hz to 1 MHz) [24, 25]. Therefore, it is reasonable to assume that the peak is originated from the Maxwell–Wagner polarization, the grain boundary with higher resistivity. The impedance spectrum represented as Z'' versus Z', which is referred as Nyquist/Cole-Cole plot is shown in **Fig. 6**. In general, the plot would be composed of three semicircles, each semicircle representing a distinct process whose time constant is sufficiently separated from the others over the range of measurement frequencies.

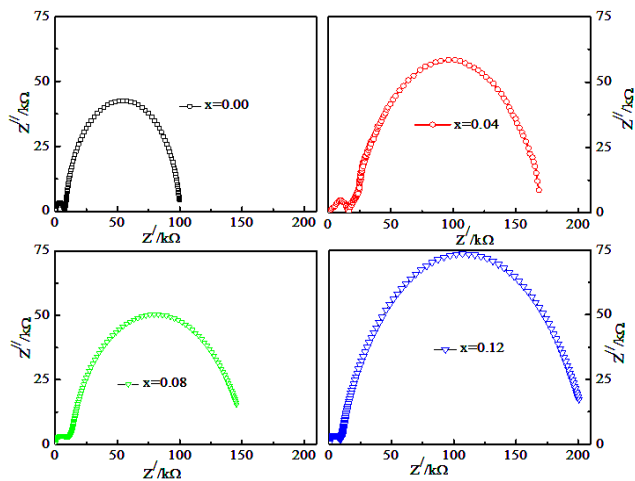**Fig. 5.** Shows the variation of Z' and Z'' (inset) with respect to the frequency.

As shown inset of **Fig. 5** similar to Z', Z'' also decreases with increasing frequency at room temperature. Two peak appeared in Z'' at low and intermediate frequency respectively. This peak proportionately shifted to lower frequency with the increase of Z'' in the low frequency region. The Z'' peak shifts to lower frequencies with

Fig. 6. Shows Cole–Cole plot for all Al ferrite compositions.

The semicircles at higher and lower frequencies represent bulk and electrode process, respectively, while that at intermediate frequencies represents grain boundary contribution [26]. In these cases, two semicircles (its tendency) are observed in the Cole–Cole plot; first semicircle at low frequency represents the resistance of the grain boundary and second semicircle obtained at high

frequency corresponds to the resistance of grain or bulk properties as shown in **Fig. 6**. The phenomenon is typically related to the existence of a distribution of relaxation time, which is according to the Cole–Cole type of distribution based on two-layer model, in which the resulting complex impedance is composed of two adjacent/overlapping semicircles depending on the relaxation time difference. A ferrite material is assumed to be consisting of piled up crystalline plates. From the microstructural point of view, a sample is assumed as a microstructure made up of parallel conducting plates (grains) separated by resistive plates (grain boundaries) [**26**]. As there is no presence of third semicircle from the contribution of electrode process in the impedance spectrum which ultimately gives the accuracy of contact in the measurement.

The Cole-Cole plots for $Ni_{0.27}Cu_{0.10}Zn_{0.63}Al_xFe_{2-x}O_4$ were recorded at room temperature. In the present investigation, flat semicircle observed for each sample between the frequency range 20 Hz–120 MHz. The size of the semicircle changes with grain size and the grain boundary. The presence of two semicircular arc obtained at higher and lower frequencies corresponds to electrical conduction by the interior of the bulk grain (G) and grain boundary (Gb) respectively. The diameter of the larger and smaller semicircle corresponds to the resistance of the Gb and G respectively [**27**]. As the Al content increases, the diameter of the semicircle increases, indicating a larger of the Gb and G interior resistance. Thus, the Z' (the real axis intercepts at low and high frequency side) and Z'' of all samples is increased with increase in Al content. The variation of G and Gb with Al content are listed in **Table 2**. From the **Table 2** it is clear that both G and G_b increases with increasing Al content. Also, the relaxation time constant ($\tau = RC$) for both grain and grain boundary, were evaluated from Z'–Z'' plot for all the composition of $Ni_{0.27}Cu_{0.10}Zn_{0.63}Al_xFe_{2-x}O_4$ and its variation with Al content given in **Table 2**. It is seen that the τ varies with substitution of Al content.

Table 2. Values of grain and grain boundary resistance and relaxation time respectively for $Ni_{0.27}Cu_{0.10}Zn_{0.63}Al_xFe_{2-x}O_4$.

Content, x	0.00	0.04	0.08	0.12
Gb (kΩ)	92.34	152.07	138.19	190.46
G (kΩ)	7.48	15.62	10.13	8.86
$\square_{gb}$ (ms)	0.16	0.22	0.16	0.17
$\square_b$ (ns)	14.3	31.6	28.1	11.1

Conclusion

Effect the $Ni_{0.27}Cu_{0.10}Zn_{0.63}Al_xFe_{2-x}O_4$ ($0 \leq x \leq 0.12$ with step of 0.04) ferrites were prepared by high temperature sintering using auto combustion precursors. X-ray analysis exhibits the spine crystal structure of the compound at room temperature. Surface morphology reveals that Al substitution reduces the average grain size from 17 μm to 12 μm and the volatilization of Zn. The real and imaginary parts of the impedance have been found to decrease with increasing frequency. Single arc with double semicircles (or tendency) obtained at room temperature corresponding to pure NiCuZn and Al substituted compositions in both the complex impedance and modulus plots suggests the single

phase character of the materials. The impedance analysis has indicated the presence of mainly grain and grain boundary contributions in the materials where both are found to increase from 7.48 kΩ to 15.62 kΩ and 92.34 kΩ to 192.46 kΩ respectively with the increase in Al content. The complex modulus plots have indicated the presence of grain boundary (tendency) along with the bulk contributions in the materials. Also, the impedance as well as modulus analysis has confirmed the presence of non-Debye type of relaxation in Al substituted NiCuZn ferrites.

Reference

1. Brabers, V.A.M. Progress in Spinel Ferrite Research, In Handbook of Magnetic Materials; vol. 8, Buschow, K. H. J. (Eds.); *Elsevier Science B.V*., North-Holland, **1995**, 189-217.
2. Cullity, B.D. Introduction to Magnetic Materials, Addison-Wesley, New York, **1972**.
3. Sugimoto, M. *J. Am. Ceram. Soc.* **1999**, *82*, 269.
   DOI: 10.1111/j.1551-2916.1999.tb20058.x
4. Valenzuela, R. *Phys. Re*s. *International*, **2012**, 591839.
   DOI: 10.1155/2012/591839
5. Verma, A.; Goel, T.C.; Mendiratta, R.G.; Alam, M.I. *Mater. Sci. Eng. B* **1999**, *60*, 156.
   PII: S0921-5107(99)00019-7
6. Aravind, G.; Gaffoor, A.; Ravinder, D.; Nathanial, V. *Adv. Mater. Lett.* **2015**, *6(2)*, 179.
   DOI: 10.5185/amlett.2015.5610
7. Dais, A.; Moreira, R.L. *Mater. Lett.* **1999**, *39*, 69.
   PII: S0167-577X(98)00219-5
8. Ranjan, R., Kumar, N., Behera, B., Choudhary, R.N.P. *Adv. Mat. Lett.* **2014**, *5*, 138.
   DOI: 10.5185/amlett.2013.fdm.52
9. Mekap, Anita, Das, Piyush R., Choudhary, R.N.P., *Adv. Mat. Lett.* **2014**, *5*, 152.
   DOI: 10.5185/amlett.2013.fdm.65
10. Ahmadu, U.; Tomas, Ŝ.; Jonah, S.A.; Musa, A.O.; Rabiu, N. *Adv. Mat. Lett.* **2013**, *4(3)*, 185.
    DOI: 10.5185/amlett.2012.7396
11. Sutar, B.C.; Das, Piyush R.; Choudhary, R.N.P. *Adv. Mat. Lett.* **2014**, *5(3)*, 131.
    DOI: 10.5185/amlett.2013.fdm.51
12. Pandey, M.; Joshi, Girish M.; Deshmukh, K.; Ahmad, *J. Adv. Mater. Lett.* **2015**, *6(2)*, 165.
    DOI: 10.5185/amlett.2015.5639
13. Batoo, K.M.; Ansari, M.H. *Nanoscale Res. Lett.* **2012**, *7:112*, 1.
    DOI: 10.1186/1556-276X-7-112
14. Kumar, S.; Alimuddin, Kumar, R.; Dogra, A.; Reddy, V.R.; Banerjee, A. *J. Appl. Phys.* **2006**, *99,* 08M910.
    DOI: 10.1063/1.2172220
15. Gul, I.H.; Maqsood, A.; Naeem, M.; Ashiq, M.N. *J. Alloy. Comp.* **2010**, *507*, 201.
    DOI: 10.1016/j.jallcom.2010.07.155
16. Hossen, M.B.; Hossain, A.K.M.A. *Proc. of IEEE Intl. Conf. on Informatics, Electronics & Vision* **2012**, 903.
    DOI: 10.1109/ICIEV.2012.6317504
17. Kumar, G.; Rani, R.; Singh, V.; Sharma, S.; Batoo, K.M.; Singh, M. *Adv. Mat. Lett.* **2013**, *4*, 682.
    DOI: 10.5185/amlett.2013.fdm.65
18. Hossen, M.B.; Hossain, A.K.M.A. *J. Magn. Magn. Mater.* **2015**, *387*, 24.
    DOI: 10.1016/j.jmmm.2015.03.083
19. Victor, P.; Bhattacharyya, S.; Krupanidhi, S.B. *J. Appl. Phys.* **2003**, *94*, 5135.
    DOI: 10.1063/1.1606509
20. Suchanicz, J. *Mater. Sci. Eng. B* **1998**, *55*,114.
    DOI: 10.1016/S0921-5107(98)00188-3.

21. Padhee, R.; Das, Piyush R.; Parida, B.N.; Choudhary, R.N.P., *J. Mater. Sci: Mater. Electron* **2012**, *23*, 1688.
    DOI: 10.1007/s10854-012-0647-3
22. Jonscher, A.K. *Nature* **1977**, *267*, 673.
    DOI: 10.1038/267673a0
23. Sen, S.; Chowdhary, R.N.P.; Tarafdar, A.; Pramanik, P. *J. Appl. Phys.* **2006**, *99*, 124114.
    DOI: 10.1016/j.physb.2006.03.028
24. Ortega, N.; Kumar, A.; Katiyar, R.S.; Scott, J.F. *Appl. Phys. Lett.* **2007**, *91*, 102902.
    DOI: 10.1063/1.2779853
25. Zhang, J.X.; Dai, J.Y.; Chan, H.L.W. *J. Appl. Phys.* **2010**, *107*, 104105.
    DOI: 10.1063/1.3386510
26. Hashim, M.; Alimuddin, Kumar, S.; Ali, S.; Koo, B.H.; Chung, H.; Kumar, R. *J. Alloy. Comp.* **2012**, *511*, 107.
    DOI: 10.1016/j.jallcom.2011.08.096
27. Kambale, R.C.; Shaikh, P.A.; Bhosale, C.H.; Rajpure, K.Y.; Kolekar, Y.D. *Smart. Mater. Struct.* **2009**, *18*, 085014.
    DOI: 10.1088/0964-1726/18/8/085014

Advanced Materials Letters

Copyright © VBRI Press AB, Sweden
www.vbripress.com

Publish your article in this journal

Advanced Materials Letters is an official international journal of International Association of Advanced Materials (IAAM, www.iaamonline.org) published by VBRI Press AB, Sweden monthly. The journal is intended to provide top-quality peer-review articles in the fascinating field of materials science and technology particularly in the area of structure, sysnthesis and processing, characterisation, advanced-sate properties, and application of materials. All published articles are indexed in various databases and are available download for free. The manuscript management system is completely electronic and has fast and fair peer-review process. The journal includes review article, research article, notes, letter to editor and short communications.